Journal of Solid State Chemistry 183 (2010) 2426–2431

Contents lists available at ScienceDirect

Journal of Solid State Chemistry

journal homepage: www.elsevier.com/locate/jssc

Oxygen-permeable membranes based on partially *B*-site substituted $BaFe_{1-y}M_yO_{3-\delta}$ (M=Cu or Ni)

Tetsuya Kida [a,*], Atsunori Yamasaki [b], Ken Watanabe [c], Noboru Yamazoe [a], Kengo Shimanoe [a]

[a] Department of Energy and Material Sciences, Faculty of Engineering Sciences, Kyushu University, Kasuga-Koen 6-1, Kasuga-shi, Fukuoka 816 8580, Japan
[b] Department of Molecular and Material Sciences, Interdisciplinary Graduate School of Engineering Science, Kyushu University, Kasuga-Koen 6-1, Kasuga-shi, Fukuoka 816 8580, Japan
[c] Sensor Materials Center, National Institute of Materials Science (NIMS), Namiki 1-1, Tsukuba, Ibaraki 305 0044, Japan

ARTICLE INFO

Article history:
Received 14 May 2010
Received in revised form
28 July 2010
Accepted 1 August 2010
Available online 5 August 2010

Keywords:
Perovskite
Oxygen permeation
Cubic structure
$BaFeO_{3-\delta}$
Partial substitution

ABSTRACT

We carried out the partial substitution of the *B*-site in $BaFeO_{3-\delta}$ perovskite with divalent cations to develop novel oxygen-permeable materials. We demonstrated that the partial substitution of Cu or Ni by more than 10% resulted in the stabilization of the cubic perovskite structure even at room temperature in a highly oxygen-permeable phase, as revealed by the X-ray diffraction (XRD) analysis. The Cu substitution was more effective for the stabilization, because the introduction of Cu in the lattice more effectively made the Goldschmidt tolerance factor (t) close to 1.0. Ni- and Cu-substituted $BaFeO_{3-\delta}$ membranes showed higher oxygen permeabilities than their parent $BaFeO_{3-\delta}$ membranes particularly at lower temperatures around 600–700 °C owing to the stabilization of the cubic phase. Among the fabricated membranes, a $BaFe_{0.85}Cu_{0.15}O_{3-\delta}$ membrane (1.0 mm thickness) showed the highest oxygen permeation flux (1.8 $cm^3\ min^{-1}\ cm^{-2}$ at 930 °C) under an air/He gradient. The results indicated that Cu-substituted $BaFeO_{3-\delta}$ is promising as a material for Co-free membranes with high oxygen permeabilities.

1. Introduction

Oxygen permeation through ceramic membranes based on mixed electron–ion conducting materials, which can be utilized for selective separation of oxygen from air to produce oxygen-enriched air, has attracted technological and scientific interest since the discovery of the phenomenon [1]. Among oxygen permeation materials developed thus far, a variety of Co-based membranes such as $SrCo_{1-y}Fe_yO_3$ [1–3], $SrCo_{1-y}Nb_yO_3$ [4], and $Ba_{1-x}Sr_xCo_{1-y}Fe_yO_3$ [5] are the most promising in terms of their high oxygen permeabilities.

Recently, we developed another series of oxygen-permeable membranes based on Fe-based perovskite-type oxides. We showed that partially *A*- or *B*-site substituted $BaFeO_{3-\delta}$ such as $Ba_{1-x}La_xFeO_{3-\delta}$ [6] and $BaFe_{1-y}Zr_yO_{3-\delta}$ [7] have high oxygen permeabilities, even at lower temperatures around 700 °C. Co-free $BaFeO_{3-\delta}$-based membranes are preferable in terms of low cost and high stabilities under reducing atmospheres. It is known that $BaFeO_{3-\delta}$ transforms its crystal structure depending on the oxygen vacancy concentration in its lattice; it forms 6H- and 12H-type hexagonal structures for $\delta \leq 0.35$, but transforms into a cubic structure for higher δ values [8–10]. These δ values are dependent on the temperature and atmospheric pressure. In the 6H-type structure, face-shared double FeO_6 octahedra are corner-linked to a single FeO_6 octahedron, as shown in Fig. 1 [9,11], which is in striking contrast to the cubic structure, wherein each FeO_6 octahedron is three-dimensionally corner-linked. It has been reported that $BaFeO_{3-\delta}$ shows almost no oxygen permeability below the temperature, at which phase transition starts to occur [6,7]. However, the thermal desorption of oxygen from the $BaFeO_{3-\delta}$ lattice at higher temperatures results in the formation of the cubic phase, significantly improving the oxygen permeability [6,7]. The difference in the oxygen permeability of $BaFeO_{3-\delta}$ between the two phases is probably, due to a significantly lower mobility of oxygen ions in the hexagonal structure than in the cubic structure having three-dimensional oxygen diffusion paths, as shown in Fig. 1. Thus, the improved performance of the partially *A*- or *B*-site substituted $BaFeO_{3-\delta}$ is likely due to the successful stabilization of the cubic perovskite phase by the proper introduction of substituting cations in $BaFeO_{3-\delta}$.

It is well accepted that for ABO_3 perovskites, the cubic phase is stable under the condition that the Goldschmidt tolerance factor (t), expressed as follows, is in the range $0.75 < t < 1.0$

$$t = \frac{(r_A + r_O)}{\sqrt{2}(r_B + r_O)} \quad (1)$$

* Corresponding author.
E-mail address: kida@mm.kyushu-u.ac.jp (T. Kida).

0022-4596/$ - see front matter © 2010 Elsevier Inc. All rights reserved.
doi:10.1016/j.jssc.2010.08.002

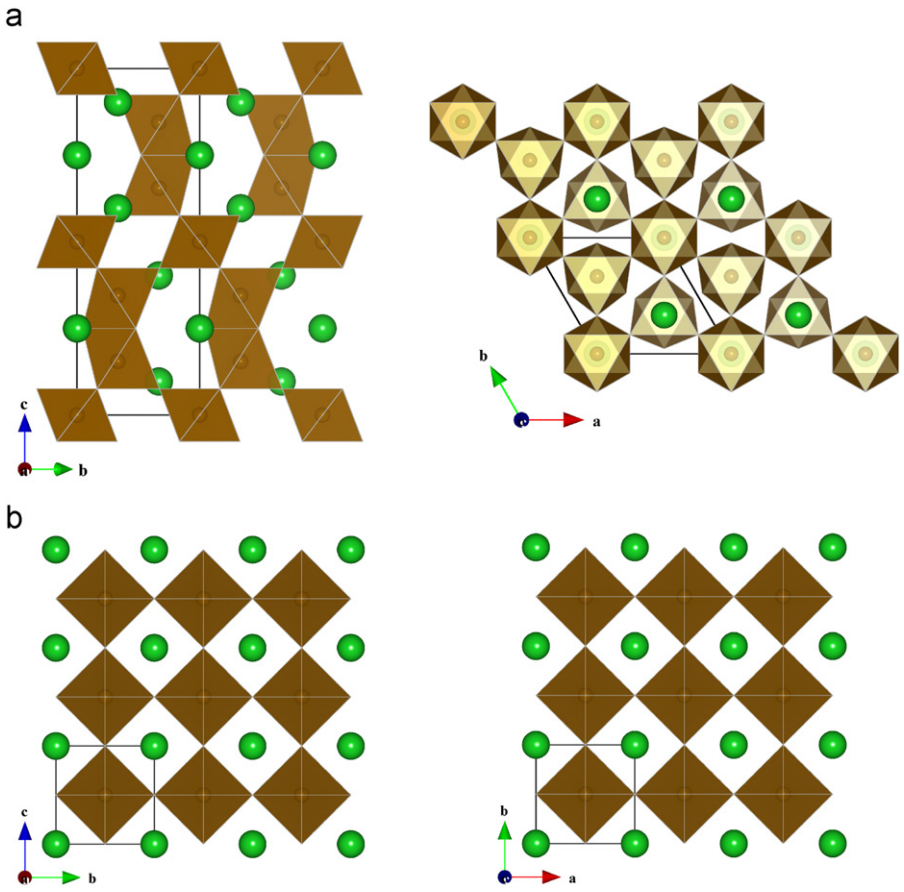

Fig. 1. Crystal structures of (a) 6H-type hexagonal $BaFeO_{3-\delta}$ (space group: *P63/mmc*; lattice constants: $a=5.683$ Å, $c=13.916$ Å [11]) and (b) ideal cubic perovskite (space group: *Pm-3m*; lattice constant: $a=4.020$ Å). Octahedra and green balls represent FeO_6 units and Ba ions, respectively. The crystal structures were drawn with VENUS, 3D visualization software developed by Dilanian and Izumi.

where r_A, r_B, and r_O are the radii of the *A*-site cation, *B*-site cation, and oxide ion, respectively. For $BaFeO_{3-\delta}$, t is estimated to be 1.066, slightly larger than the optimum value. This is due to the relatively large ionic radius of Ba. Thus, the replacement of *A*- or *B*-site with smaller or larger cations, respectively, would stabilize the cubic perovskite structure. Indeed, the partial replacement of *A*- or *B*-site in $BaFeO_{3-\delta}$ with Sr [12] or Ce [13], respectively, has been shown to be effective for the stabilization. The reported results suggest the possibility of further upgrading the oxygen permeability of $BaFeO_{3-\delta}$-based membranes via an optimized composition control.

In this study, we selected divalent Ni^{2+} (0.69 Å) and Cu^{2+} (0.73 Å) as substituting cations, because of their larger ionic radii than those of Fe^{3+} (0.55 Å) and Fe^{4+} (0.585 Å). Furthermore, for Fe sites, the substitution of divalent cations should increase the oxygen vacancy concentration in the lattice via charge compensation. The doping of Cu [4,14–17] or Ni [14,17–20] into Co-, Ti-, and Ga-based perovskite-type oxides has already been demonstrated to yield improved oxygen permeabilities. Here, we show the oxygen permeability of the partially *B*-site substituted $BaFe_{1-y}M_yO_{3-\delta}$ (M=Cu or Ni) along with the effect of partial substitution of Cu or Ni on the crystal structure.

2. Experimental

We prepared $BaFe_{1-y}M_yO_{3-\delta}$ (M=Cu, Ni; y=0–0.15) powders by a pyrolysis method as follows. The constituting metal nitrates or acetates were dissolved in water and the resultant solution was evaporated to dryness at 350 °C. The dried powder was calcined at 850 °C for 5 h in air. Then, we ground and crushed the calcined powder in ethanol with a planet-type ball-mill for 15 h. After drying, the ball-milled powders were press-formed at 4.0 MPa into a disk (diameter: 2 cm), and then sintered at from 1020 to 1175 °C for 5 h in air. The sintering temperature depended on membrane composition, as shown in Table 1. For sintering, the cooling and heating rates were set to 2 and 4 °C min^{-1}, respectively. The above procedure yielded well-sintered membranes, as shown in the optical images of representative membranes (Fig. 2). Nitrogen permeation tests also confirmed their gas tightness.

The crystal structures of the obtained membranes were characterized on a high-temperature X-ray diffractometer (HT-

Table 1
Sintering temperature of fabricated membranes.

Sample no.	Composition	Sintering temperature/°C
1	$BaFe_{0.975}Ni_{0.025}O_{3-\delta}$	1020
2	$BaFe_{0.95}Ni_{0.05}O_{3-\delta}$	1020
3	$BaFe_{0.9}Ni_{0.1}O_{3-\delta}$	1150
4	$BaFe_{0.85}Ni_{0.15}O_{3-\delta}$	1175
5	$BaFe_{0.95}Cu_{0.05}O_{3-\delta}$	1175
6	$BaFe_{0.9}Cu_{0.1}O_{3-\delta}$	1175
7	$BaFe_{0.85}Cu_{0.15}O_{3-\delta}$	1075

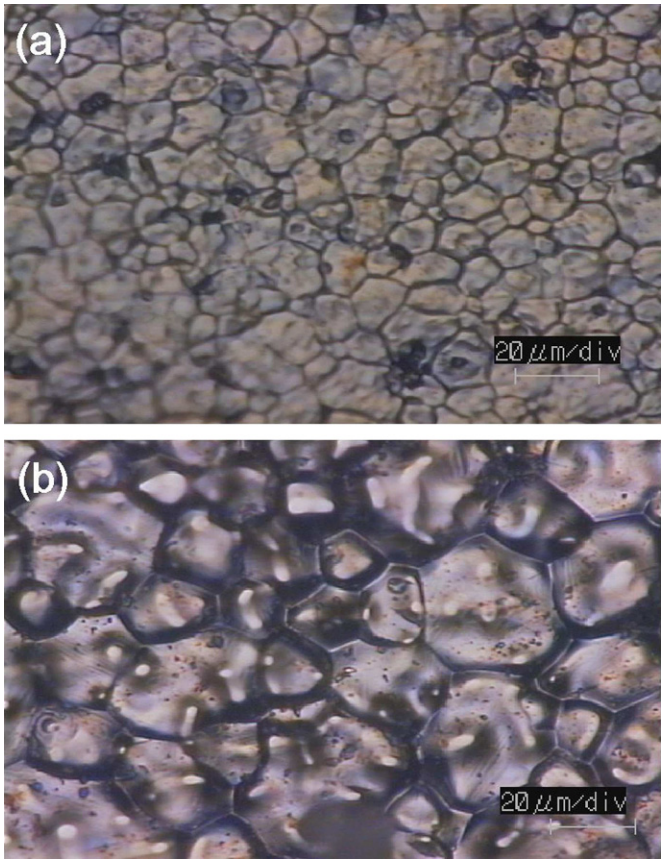

Fig. 2. Optical microscope images of (a) $BaFe_{0.85}Ni_{0.15}O_{3-\delta}$ and (b) $BaFe_{0.85}Cu_{0.15}O_{3-\delta}$ membranes.

XRD), using Cu Kα radiation (RINT2100, Rigaku Co., Ltd.) from room temperature (RT) to 900 °C. For XRD measurements, sample disks fabricated at 1020–1175 °C were used, and the scan rate was set as 2° min^{-1}. For HT-XRD measurements, the temperature was slowly increased from RT to 600, 700, 800, and 900 °C and was maintained constant at each designated temperature for more than 1 h before measurements were taken.

The oxygen permeability through the membranes was measured, using an apparatus reported elsewhere [7]. The surface of the membranes was polished with an emery paper (#80) to adjust their thicknesses to 1.0 mm and to reduce or eliminate any surface effects on the oxygen permeation, through differences in the membranes, by controlling their surface porosities with the same conditions. We fixed the membrane to a quartz tube by welding with a silver ring at 960–965 °C. For permeation tests, synthetic air (200 cm^3 min^{-1}) and He (150 cm^3 min^{-1}) were each flowed to one side of the membrane. The oxygen concentration in the He flow was below 0.05 ppm. We monitored the amount of oxygen passing through the membrane from the air side to the He side, using a thermal conductivity detector (TCD) connected to a gas chromatography system. The measurement was performed at 530–930 °C.

We used a temperature-programmed desorption (TPD) technique to examine the oxygen desorption properties of the $BaFe_{1-y}M_yO_{3-\delta}$ powders. A sample powder (1.0 g) was embedded in glass–wool packed in a quartz reactor, heat-treated at 1000 °C for 1 h under a flow of synthetic air (50 mL min^{-1}), and then cooled to RT in the same atmosphere. After switching the atmosphere to a helium flow (50 mL min^{-1}), the sample was heated at a constant rate of 10 °C min^{-1} and the oxygen desorbed was monitored using a TCD.

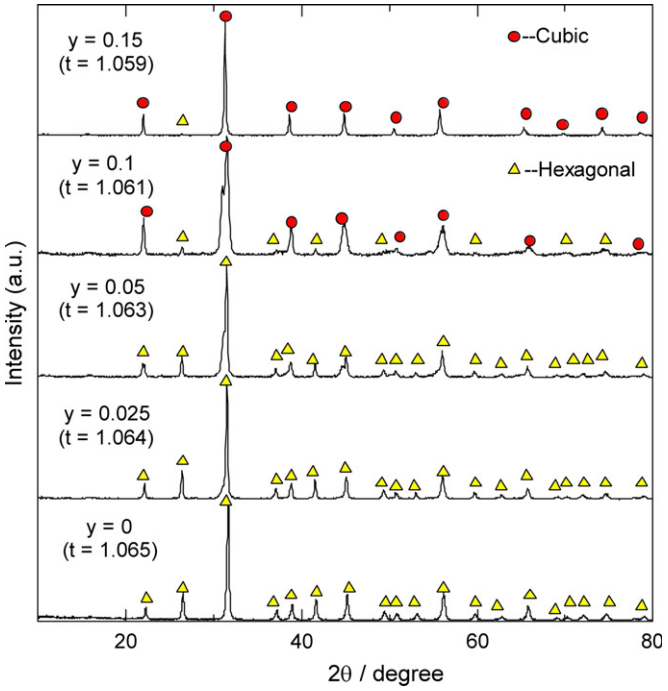

Fig. 3. XRD patterns of $BaFe_{1-y}Ni_yO_{3-\delta}$ (y=0–0.15) membranes. The tolerance factor (t) is noted in parentheses.

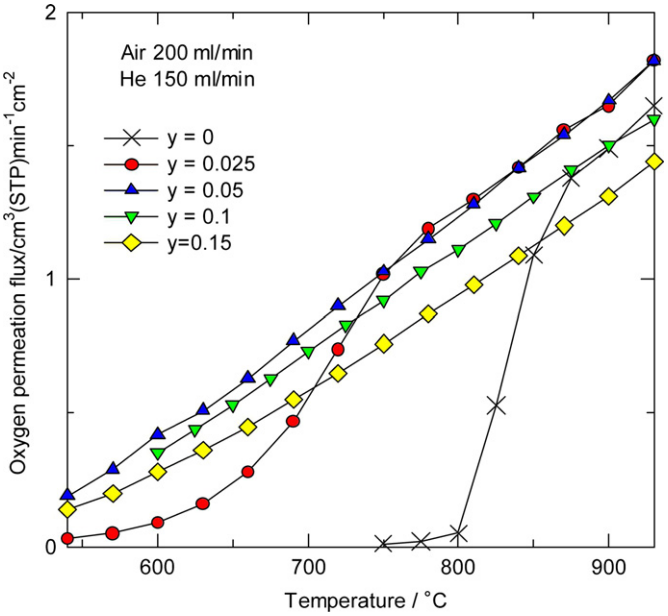

Fig. 4. Oxygen permeability of $BaFe_{1-y}Ni_yO_{3-\delta}$ (y=0–0.15) membranes (1.0 mm thickness) as a function of temperature.

3. Results and discussion

3.1. Crystal structure and oxygen permeability of $BaFe_{1-y}Ni_yO_{3-\delta}$

Fig. 3 shows the XRD patterns of $BaFe_{1-y}Ni_yO_{3-\delta}$ (y=0–0.15) membranes along with their tolerance factors. The crystal structure of the parent $BaFeO_{3-\delta}$ (y=0) can be assigned to a hexagonal phase, as reported in the literature [11]. The crystal structure remained unchanged in the substitution range y=0.025–0.05, but the cubic phase appeared in the substitution range y=0.1–0.15. The formation of the cubic phase after

increasing the substitution amount is likely due to a decrease in t. However, the peak ascribable to the hexagonal phase remained in the XRD pattern, even at the highest substitution amount ($y=0.15$). No impurity phases were detected in these patterns.

Fig. 4 shows the oxygen permeation fluxes of $BaFe_{1-y}Ni_yO_{3-\delta}$ ($y=0$–0.15) membranes (1 mm thickness) as a function of temperature. The oxygen permeability of the parent $BaFeO_{3-\delta}$ was almost negligible below 800 °C, but abruptly increased around 800 °C due to phase transition from hexagonal to triclinic and cubic structures, as confirmed by the HT-XRD analysis [6]. The trend of the oxygen permeation through $BaFeO_{3-\delta}$ as a function of temperature was rather different from the reported results, where a slight change in the composition, particularly in the oxygen content, might induce this difference. In contrast, the membrane with the lowest Ni substitution amount ($y=0.025$) showed a gradual change in the oxygen permeability around 700 °C. In contrast, the membranes with higher Ni substitution amounts ($y=0.05$–0.15) showed no such abrupt changes in the oxygen permeation flux. For the membranes with $y=0.1$ and 0.15, the cubic phase stabilized even at RT, as shown in Fig. 3. The cubic phase stabilization should increase the oxygen permeability particularly at lower temperatures. However, the membranes with $y=0.025$ and 0.05 also showed improved oxygen permeability, although they had hexagonal phases that might have fewer paths for oxide ion diffusion. Thus, it is possible that the phase transformation from hexagonal to cubic phase occurred for Ni-substituted membranes with $y=0.025$ and 0.05.

To obtain experimental proof for the above idea, we examined the crystal structure of $BaFe_{0.95}Ni_{0.05}O_{3-\delta}$ ($y=0.05$) using HT-XRD, as shown in Fig. 5. The membrane showed the cubic structure from 600 to 900 °C, without detectable peaks ascribable to the hexagonal phase. The results indicated the stabilization of the cubic phase at moderately high temperatures via the introduction of a small amount of Ni into the lattice. The Ni introduction likely lowered the phase transformation temperature of $BaFeO_{3-\delta}$ from around 800 °C to below 600 °C. However, note that the increase in the Ni substitution amount degraded the oxygen permeability, as observed for membranes with $y=0.1$ and 0.15. This result is contradicted by the fact that the cubic phase stabilized even at RT and by the expectation that the oxygen vacancy concentration increased via the larger Ni substitution. The exact reasons for these findings are not yet clear, but the formation of undetectable impurity phases at the grain boundary or a change in the oxide-ion mobility after introduction of larger amounts of Ni might decrease the oxygen permeability.

3.2. Crystal structure and oxygen permeability of $BaFe_{1-y}Cu_yO_{3-\delta}$

Fig. 6 shows the XRD patterns of $BaFe_{1-y}Cu_yO_{3-\delta}$ ($y=0$–0.15) membranes along with their tolerance factors. As seen for the Ni-substituted membranes, the crystal structure remained unchanged at a lower substitution amount ($y=0.05$), but an increase in the substitution amount ($y=0.1$–0.15) successfully stabilized the cubic phase. The stabilization was accompanied by a decrease in t, as in the case for an Ni substitution. Preferably, for the higher Cu substitution, no peaks ascribable to the hexagonal phase were detected in the XRD patterns, which is in contrast to the Ni substitution. The results indicated an enhanced effect of Cu substitution on the cubic phase stabilization, because the substitution of Cu more effectively made t close to 1.0 even with a smaller amount of substitution, because of its larger ionic radius as compared with Ni. However, further introduction of Cu failed to obtain dense-disk membranes, because of the melting of the membranes.

Fig. 7 shows the oxygen permeation fluxes of $BaFe_{1-y}Cu_yO_{3-\delta}$ ($y=0$–0.15) membranes (1 mm thickness) as a function of temperature. All membranes showed higher oxygen permeabilities than the original membrane ($y=0$), particularly at lower temperatures around 600–700 °C. The membrane with a lower Cu substitution amount ($y=0.05$), which had a hexagonal structure at RT, also showed improved oxygen permeability. The phase transition from hexagonal to cubic phases occurred below 600 °C, as in the above case for membranes with lower Ni substitution amounts. All Cu-substituted membranes showed similar oxygen permeabilities, although we observed slight increases in the oxygen permeation fluxes at the highest substitution amount ($y=0.15$). The obtained oxygen permeation fluxes were higher than those of the Ni-substituted membranes, indicating the more effective role of Cu in stabilizing the cubic perovskite structure even with lower substitution amounts.

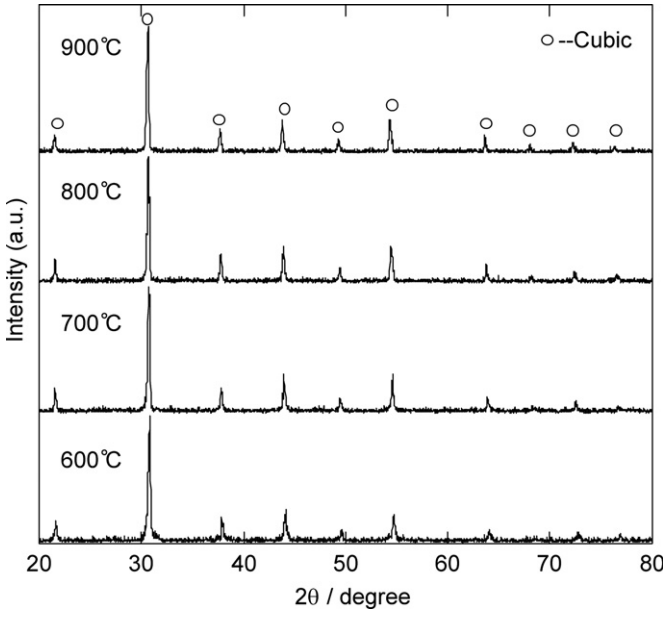

Fig. 5. HT-XRD patterns of a $BaFe_{0.95}Ni_{0.05}O_{3-\delta}$ membrane ($y=0.05$) from 600 to 900 °C.

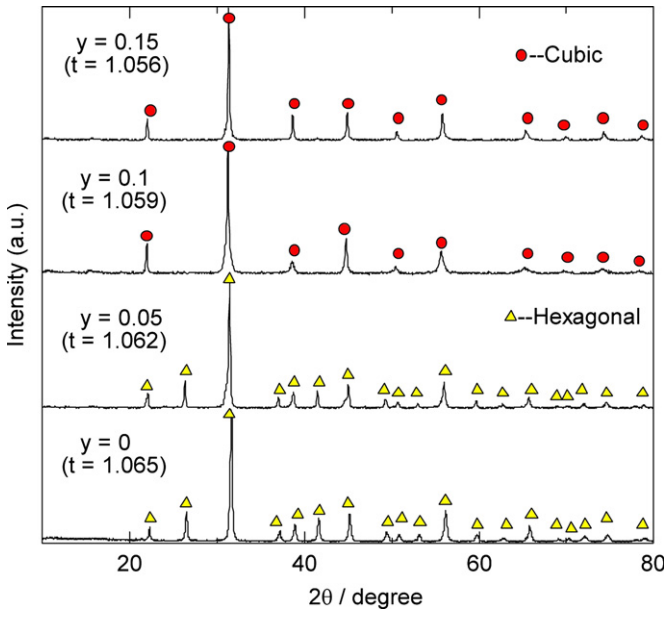

Fig. 6. XRD patterns of $BaFe_{1-y}Cu_yO_{3-\delta}$ ($y=0$–0.15) membranes. The tolerance factor (t) is noted in parentheses.

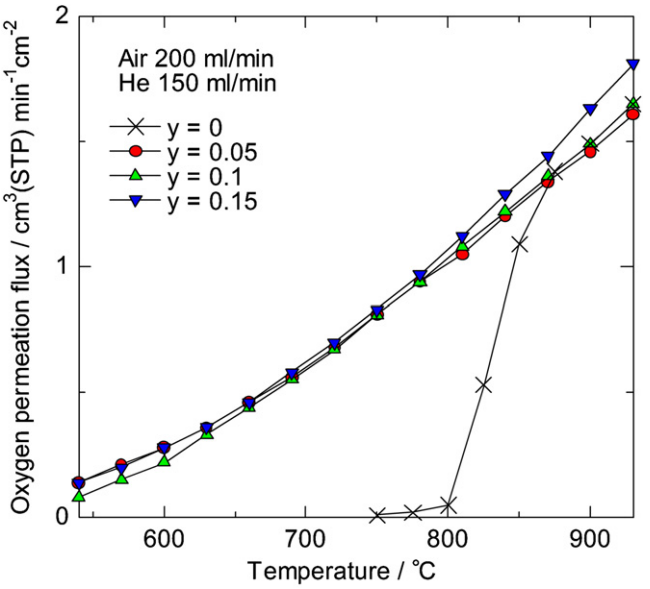

Fig. 7. Oxygen permeabilities of $BaFe_{1-y}Cu_yO_{3-\delta}$ (y=0–0.15) membranes (1.0 mm thickness) as a function of temperature.

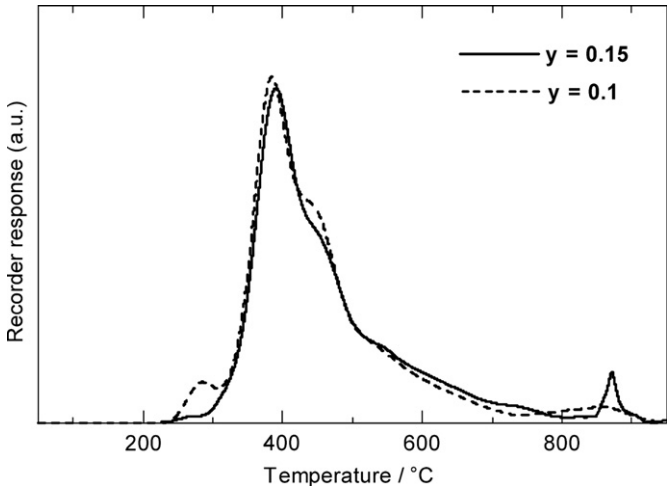

Fig. 8. TPD chromatograms of oxygen from $BaFe_{1-y}Cu_yO_{3-\delta}$ (y=0.1 and 0.15) powders.

TPD measurements provide very useful information on the oxygen sorptive–desorptive properties of membranes [21–23]. To confirm the high oxygen permeation properties of Cu-substituted membranes, we investigated the temperature-dependent oxygen desorption from the membranes, using the TPD technique. Fig. 8 shows the TPD chromatograms of oxygen from the $BaFe_{1-y}Cu_yO_{3-\delta}$ (y=0.1 and 0.15) powders. The chromatograms were characterized by the appearance of two oxygen desorption peaks, denoted as α and β, at lower (200–700 °C) and higher (700–900 °C) temperature regions, respectively. It has been reported that for Co and/or Fe-containing perovskite-type oxides, α desorption corresponds to the desorption of oxygen incorporated in oxygen vacancies in the lattice, accompanied by the reduction of Co^{4+} (and/or Fe^{4+}) to Co^{3+} (and/or Fe^{3+}). In contrast, β desorption corresponds to the reduction of Co^{3+} (and/or Fe^{3+}) to Co^{2+} (and/or Fe^{2+}) [22,24,25]. Thus, for $BaFeO_{3-\delta}$-based membranes, α and β desorptions are associated with the reduction of Fe^{4+} to Fe^{3+} and Fe^{3+} to Fe^{2+}, respectively. It is possible that the reduction of Cu^{2+} to Cu^{+} also took place in β desorption, particularly for the membrane with a higher Cu substitution amount, as shown by a sharp β peak in its TPD chromatograph. Also, β desorption at 700–900 °C associated with the reduction of Cu^{2+} to Cu^{+} has been reported for Cu-doped ceria [26] and Cu-doped $LaCoO_3$ [27].

The oxygen desorption started to occur near 200 °C, which is quite low as compared with Co-containing membranes. The total amounts of oxygen desorbed were 381 and 368 μmol g^{-1} for $BaFe_{0.9}Cu_{0.1}O_{3-\delta}$ and $BaFe_{0.85}Cu_{0.15}O_{3-\delta}$, respectively, which are far larger values than those obtained for a surface monolayer. These results indicated that oxygen was desorbed mainly from the bulk. The observation of large α desorption peaks was a clear indication that the membranes contained a large amount of oxygen vacancies even at lower temperatures. These vacancies must be responsible for the enhancement of the oxygen permeation fluxes at lower temperatures. Note that there was no significant difference in the shape of the α desorption peaks and the amounts of desorbed oxygen between the two membranes with different Cu substitution amounts (y=0.1 and 0.15). Similar oxygen sorptive–desorptive properties likely resulted in no significant difference in the oxygen permeabilities between the two membranes. However, a slight increase in permeation fluxes around 900 °C was observed with the highest Cu substitution (y=0.15), as noted above. This result might be due to the creation of additional oxygen vacancies in the lattice, resulting from the reduction of Cu^{2+} to Cu^{+} (β desorption) around 900 °C.

The obtained results indicated that Cu-substituted $BaFeO_{3-\delta}$ is promising for Co-free, cheap oxygen-permeable membranes with high performance. The $BaFe_{0.85}Cu_{0.15}O_{3-\delta}$ membrane showed the highest oxygen permeation flux of 1.8 cm^3 (standard temperature pressure) min^{-1} cm^{-2} at 930 °C under an air/He gradient, a value comparable with those for Co-based membranes. In addition, the obtained permeation fluxes for Cu and Ni-substituted membranes were similar to those obtained for Zr- and La-substituted $BaFeO_{3-\delta}$ membranes [6,7], thus confirming an effective material design of partial *A*- and/or *B*-site substitution in $BaFeO_{3-\delta}$ with other cations. Although the Ni-substituted membranes showed comparably high oxygen permeation fluxes, they experienced a phase transition from hexagonal to cubic phases. We expected the phase transition to bring about shrinkage and expansion of the membranes, resulting in the degradation of their stabilities during heat cycle operation. Thus, the stabilization of the cubic perovskite structure and suppression of the phase transition via Cu substitution are preferable for the stability of the membranes. However, the introduction of a larger amount of Cu would degrade the stability due to the reduction of $Cu^{2+}$to Cu^{+} at elevated temperatures. Further optimization of the membrane composition is necessary for the improvement of their stabilities for practical use.

Another way of improving the oxygen permeability is by controlling the microstructure of these membranes. We previously reported that the oxygen permeability of $Ba_{0.95}La_{0.05}FeO_{3-\delta}$ membranes depended on their microstructure; a decrease in the grain size by a wet chemical method, using chelating agents, led to an improvement in the oxygen permeation fluxes [28]. Thus, microstructural control likely upgrades the performance of Cu-substituted $BaFeO_{3-\delta}$ membranes.

4. Conclusion

The partial substitution of Ni and Cu on the *B*-site in $BaFeO_{3-\delta}$ stabilized the cubic perovskite structure at RT, depending on the substitution amount. The cubic perovskite phase effectively stabilized when the substitution amount was increased, accompanied with a decrease in t. Ni- and Cu-substituted $BaFeO_{3-\delta}$ membranes showed higher oxygen permeabilities than the parent $BaFeO_{3-\delta}$ membrane, particularly at lower temperatures around

600–700 °C due to the stabilization of the cubic phase. Among the fabricated membranes, a $BaFe_{0.85}Cu_{0.15}O_{3-\delta}$ membrane (1.0 mm thickness) showed the highest oxygen permeation flux of 1.8 cm^3 (standard temperature pressure) min^{-1} cm^{-2} at 930 °C under an air/He gradient. TPD measurements revealed that Cu-substituted membranes desorbed a large amount of oxygen from the bulk at lower temperatures, which may be the reason for the high oxygen permeability at lower temperatures.

Acknowledgment

This work was supported by the Steel Industry Foundation.

References

[1] Y. Teraoka, H.-M. Zhang, S. Furukawa, N. Yamazoe, Chem. Lett. 14 (1985) 1743–1746.
[2] H. Kruidhof, H.J.M. Bouwmeester, R.H.E. Doorn, A.J. Burggraaf, Solid State Ionics 63–65 (1993) 816–822.
[3] L. Qiu, T.H. Lee, L.M. Liu, Y.L. Yang, A.J. Jacobson, Solid State Ionics 76 (1995) 321–329.
[4] T. Nagai, W. Itoh, T. Sakon, Solid State Ionics 177 (2007) 3433–3444.
[5] Z. Shao, W. Yang, Y. Cong, H. Dong, J. Tong, G. Xiong, J. Membr. Sci. 172 (2000) 177–188.
[6] K. Watanabe, D. Takauchi, M. Yuasa, T. Kida, K. Shimanoe, Y. Teraoka, N. Yamazoe, J. Electrochem. Soc. 156 (2009) E81–E85.
[7] T. Kida, K. Watanabe, D. Takauchi, M. Yuasa, K. Shimanoe, Y. Teraoka, N. Yamazoe, J. Electrochem. Soc. 156 (2009) E187–E191.
[8] M. Parras, M. Vallet-Regi, J.M. Gonzalez-Calbet, J.C. Grenier, J. Solid State Chem. 83 (1989) 121–131.
[9] J.C. Grenier, A. Wattiaux, M. Pouchard, P. Hagenmuller, M. Parras, M. Vallet, M.A. Alario-Franco, J. Solid State Chem. 80 (1989) 6–11.
[10] J.C. Grenier, L. Fournes, M. Pouchard, P. Hagenmuller, M. Parras, M. Vallet, J. Calbet, Z. Anorg. Allg. Chem. 576 (1989) 108–116.
[11] E. Lucchini, S. Meriani, D. Minichelli, Acta Cryst. B29 (1973) 1217–1219.
[12] Y. Teraoka, T. Shimokawa, C.Y. Kang, H. Kusaba, K. Sasaki, Solid State Ionics 177 (2006) 2245–2248.
[13] X. Zhu, H. Wang, W. Yang, Chem. Commun. 10 (2004) 1130–1131.
[14] Y. Teraoka, T. Nobunaga, K. Okamoto, N. Miura, N. Yamazoe, Solid State Ionics 48 (1991) 207–212.
[15] V.V. Kharton, V.N. Tikhonovich, Li Shuangbao, E.N. Naumovich, A.V. Kovalevsky, A.P. Viskup, I.A. Bashmakov, A.A. Yaremchenko, J. Electrochem. Soc. 145 (1998) 1363–1373.
[16] H. Nie, H. Zhang, G. Yu, N. Yang, Sep. Purif. Technol. 25 (2001) 415–418.
[17] H. Zhang, T. Wang, X. Dong, W. Lin, J. Nat. Gas Chem. 18 (2009) 45–49.
[18] H. Iwahara, T. Esaka, T. Mangahara, J. Appl. Electrochem. 18 (1988) 173–177.
[19] V.V. Kharton, A.V. Kovalevsky, V.N. Tikhonovich, E.N. Naumovich, A.P. Viskup, Solid State Ionics 110 (1998) 53–60.
[20] H. Arikawa, T. Yamada, T. Ishihara, H. Nishiguchi, Y. Takita, Chem. Lett. 28 (1999) 1257–1258.
[21] Y. Teraoka, M. Yoshimatsu, N. Yamazoe, T. Seiyama, Chem. Lett. 13 (1984) 893–896.
[22] Y. Teraoka, H.-M. Zhang, N. Yamazoe, Chem. Lett. 14 (1985) 1367–1370.
[23] H.-M. Zhang, N. Yamazoe, Y. Teraoka, J. Mater. Sci. Lett. 8 (1989) 995–996.
[24] Z. Shao, G. Xiong, J. Tong, H. Dong, W. Yang, Sep. Purif. Technol. 25 (2001) 419–429.
[25] L. Yang, L. Tan, X. Gu, W. Jin, L. Zhang, N. Xu, Ind. Eng. Chem. Res. 42 (2003) 2299–2305.
[26] Q. Liang, X. Wu, D. Weng, H. Xu, Catal. Today 139 (2008) 113–118.
[27] R. Zhang, A. Villanueva, H. Alamdari, S. Kaliaguine, Appl. Catal. B: Environ. 64 (2006) 220–233.
[28] K. Watanabe, S. Ninomiya, M. Yuasa, T. Kida, N. Yamazoe, H. Haneda, K. Shimanoe, J. Am. Ceram. Soc. 93 (2010) 2012–2017.